Aerosol and Air Quality Research, 17: 2129–2138, 2017

ISSN: 1680-8584 print / 2071-1409 online
doi: 10.4209/aaqr.2016.12.0593

Determination of Silt Loading Distribution Characteristics Using a Rapid Silt Loading Testing System in Tianjin, China

Wei Zhang, Yaqin Ji*, Shijian Zhang, Lei Zhang, Shibao Wang

College of Environmental Science and Engineering, Nankai University, Jinnan District, Tianjin 300350, China

ABSTRACT

Silt loading (*sL*) is an important parameter in the fugitive road dust (FRD) emission inventory because it can indicate the cleaning degree of roads. In this study, we combined Testing Re-entrained Aerosol Kinetic Emissions from Roads (TRAKER) with the AP-42 method to measure the *sL* values of paved roads in Tianjin, China, and we developed a rapid silt loading testing system for the period from January to October in 2015. This allowed us to establish the FRD *sL* reservoir in a more feasible manner on a larger urban scale compared with *sL* measurements alone. We found that the background-corrected TRAKER signals tended to increase slightly as the speed of the mobile monitoring system increased, and the *sL* values increased exponentially with the speed-corrected TRAKER signals. The *sL* values determined by TRAKER were quite different, where branch roads > minor arterials > major arterials > outer ring > expressway, due to differences in the average speed and traffic volume. Furthermore, the *sL* values determined using TRAKER were higher in the slow lanes than the other lanes (except for the outer ring), whereas the *sL* values produced by TRAKER in the express lanes of the outer ring were the highest among all the vehicle lanes. The frequency distribution of the *sL* values obtained by TRAKER for various types of roads differed significantly from each other in terms of magnitude, especially on the branch roads and minor arterials. In terms of the temporal distribution, the *sL* values obtained by TRAKER were substantially higher in summer, followed by spring and autumn, and lowest in winter.

Keywords: AP-42; Silt loading; Tianjin; TRAKER.

INTRODUCTION

The recent rapid economic growth in China has been accompanied by a severe particulate matter pollution problem. In particular, fugitive dust has attracted much attention in China because it is one of the main sources of particulate matter (Long *et al.*, 2016; Tian *et al.*, 2016). Fugitive road dust (FRD) is an important type of fugitive dust in cities (Etyemezian *et al.*, 2003; Amato *et al.*, 2009b; Li *et al.*, 2016) and one of the major contributors to particulate matter (Sun *et al.*, 2004; Zhao *et al.*, 2006; Cheng *et al.*, 2007; Thorpe and Harrison, 2008; Amato *et al.*, 2009a; Athanasopoulou *et al.*, 2010; Karanasiou *et al.*, 2011; Martuzevicius *et al.*, 2011; Amato *et al.*, 2012; Lu *et al*, 2016; Sindhwani *et al*, 2015; Zhao *et al.*, 2016). Furthermore, the contribution of FRD to the total $PM_{2.5}$ emissions is about 20% (Karagulian *et al.*, 2015; Liu *et al.*, 2015; Gao *et al.*, 2016; Hsu *et al.*, 2016; Gopinath *et al*, 2017). FRD not only affects the air quality and visibility (Almeida *et al.*, 2006; Moreno *et al.*, 2013; Cyrys *et al.*, 2014; Liu *et al.*, 2014; Amato *et al.*, 2016; Borrego *et al.*, 2016), but it is also highly detrimental to health (Lu *et al.*, 2009; Tente *et al.*, 2011; Huang *et al.*, 2014; Lai *et al.*, 2016; Sumit *et al.*, 2016). Thus, controlling and quantifying the particulate matter emissions produced by vehicle traffic and resuspended on roads is essential for understanding the potential emissions of particulate pollution, thereby establishing foundations for environmental management and managing the air quality by implementing particle matter (PM) reduction measures (Etyemezian *et al.*, 2003; Amato *et al.*, 2010; Kavouras *et al.*, 2016).

Silt loading (*sL*) is a very important parameter in the FRD emission inventory and thus for environmental management. The AP-42 method (i.e., vacuuming and sweeping) specified by the EPA has been employed by many researchers to study FRD emissions, including emission inventories, emission characteristics, and the efficiency of control measures (Fan *et al.*, 2009). However, this method is not practicable for measuring *sL* on a regional scale because of time constraints and safety problems. In particular, it cannot precisely reflect the actual situation regarding the resuspension of FRD due to vehicular travel because the resuspension mechanism assumed for FRD might not be the same as that due to actual vehicular travel (Han *et al.*, 2011).

* Corresponding author.
Tel.: +86-022-23503397; Fax: +86-22-23503397
E-mail address: jiyaqin@nankai.edu.cn

Therefore, in this study, we developed a rapid silt loading testing system by combining Testing Re-entrained Aerosol Kinetic Emissions from Roads (TRAKER) with the AP-42 method to detect the silt loading on roads in Tianjin, China. The TRAKER system was first tested in Las Vegas, USA by Kuhns *et al.* (2001). Subsequently, it was used to assess the quantitative relationships among the key factors that generated road particle emissions (Hussein *et al.*, 2008). Kwak *et al.* (2014) also utilized TRAKER to investigate the physical and chemical characteristics of ultrafine particles in Hwaseong, South Korea.

The new system has several advantages, as follows: (1) the dust emissions from long stretches and numerous roads can potentially be surveyed in a quantitative manner within a short time (Kuhns *et al.*, 2001; Han and Jung, 2012); (2) the results obtained by this system can reflect the actual FRD resuspension mechanism due to vehicles; (3) the system can perform tasks that are not possible using AP-42 alone and it is more flexible on an urban scale.

Road dust pollution is an important issue in Tianjin because of its high volume of vehicles. Various studies in this field have concentrated mostly on the FRD emission characteristics or its chemical components (Hussein *et al.*, 2008; Fan *et al.*, 2009; Zhu *et al.*, 2009; Kauhaniemi *et al.*, 2014; Kwak *et al.*, 2014), whereas few studies have considered the spatial and temporal variations in important parameters in the FRD emission inventory.

In this study, we obtained the first experimental estimates of *sL* using a rapid silt loading testing system in Tianjin. The main objective of this study was to obtain the *sL* values for all of the roads sampled by combining TRAKER with the AP-42 method. The secondary objective was to determine the spatial and temporal distribution characteristics of the *sL* values obtained by TRAKER. The final objective was to provide an experimental basis for measuring emission factors and emissions for FRD due to vehicle movements, thereby establishing an emissions inventory for FRD.

EXPERIMENTAL METHODS

Particle Concentration Monitoring System

A schematic of the sampling system is shown in Fig. 1. The vehicle used in this experiment was a four-door, four-wheel Ford Maverick vehicle (2012) with a curb weight of 2092 kg. The vehicle was equipped with a global positioning system (GPS) receiver and two DustTrak particle monitors with a 2.5 μm size selective inlet. The DustTrak particle monitor (model #8530, TSI Company, USA) is a portable instrument for measuring the concentrations of different particle sizes in real time. Before starting a test, all of the instruments were synchronized with the time reported by the GPS.

The two inlet lines of DustTrak entered the compartment of the sports-utility vehicle through the car windows, where the lines were 9 mm in diameter and 2.0 m in length. One inlet of the tire lines on the right was 175 mm above the ground and 50 mm behind the tire. Measurements obtained behind the tire while moving indicated that the air speed along the center of the tire was not influenced significantly by the ambient wind direction at distances less than 100 mm from the tire (Etyemezian *et al.*, 2003). Another inlet was placed on the roof to test the background concentrations, whereas it was laid above the hood of the vehicle in a previous study (Kuhns *et al.*, 2001) or on the front bumper (Han *et al.*, 2011). This could reduce the effects of other vehicles on the background concentration.

The DustTrak data obtained from both the roof and tire-mounted instruments were combined with the GPS data based on their common time variables. Each 1-s TRAKER data set was considered to be valid if the following criteria were satisfied: (1) the maximum threshold for acceleration and deceleration was 0.5 m s^{-2}. Braking and hard acceleration or deceleration could emit a high concentration of particulate matter instantly; (2) when the vehicle speed (measured by the GPS) was less than 5 km h^{-1}, it was assumed that the TRAKER signal was insignificant and the data were invalid;

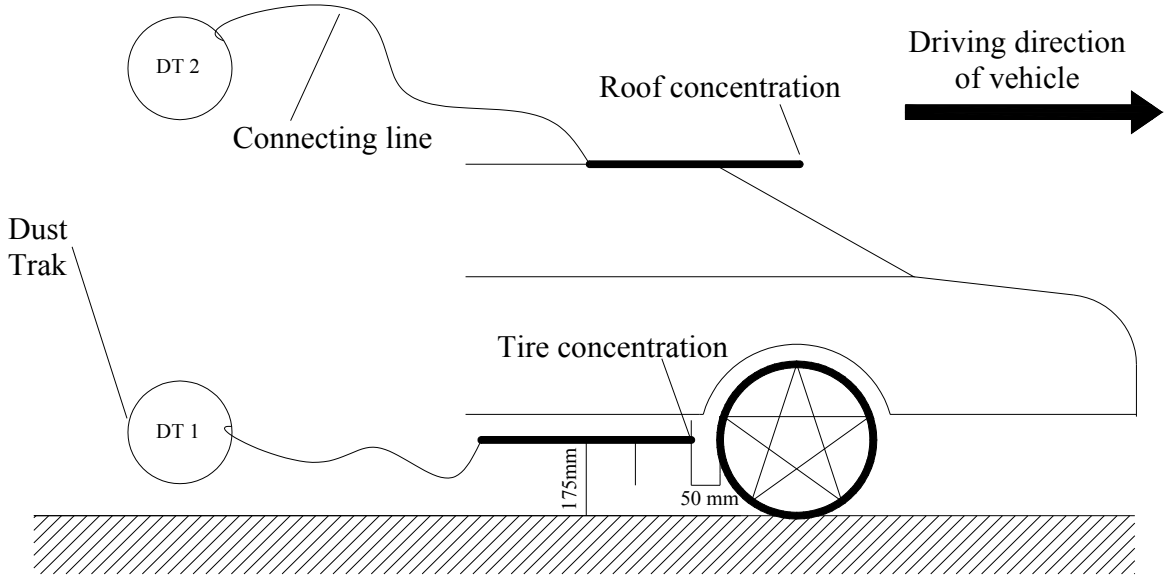

Fig. 1. Configuration of the TRAKER vehicle instrument.

(3) the maximum threshold for the wheel angle with respect to the body of the vehicle was 3°, which ensured that the orientation of the TRAKER inlets with respect to the front tire did not change during the measurements (Etyemezian *et al.*, 2003).

Speed Response

The variation in the TRAKER signals with vehicle speed was assessed during testing on paved roads in Tianjin. A straight 1200-m section of road was covered in both the eastbound and westbound directions. According to the maximum speed in the urban area (80 km h^{-1}) and the minimum threshold speed reported previously (5 m s^{-1}) (Etyemezian, 2003), four passes were completed at each speed (10, 15, 20, 25, 30, 35, 40, 45, 50, 55, 60, 65, 70, 75, and 80 km h^{-1}) with a total of 60 passes. The TRAKER signals obtained from the DustTrak were averaged for each pass.

sL Sampling System

In addition to TRAKER measurements, samples were collected from nine paved road sites during four seasons. At each site, four sections of the sampled roads were measured, marked, and vacuumed using an 800-W vacuum cleaner, 1 m^2 sampling frame, fine wool brush, 3-kw gasoline generator, and a handheld GPS receiver. The samples were weighed and sieved using a 200-mesh standard Taylor screen, a "one over ten thousand" electronic balance, and an electric vibration sieve machine. The nine paved roads comprised one expressway, one outer ring, two major arterial roads, two minor arterial roads, and three branch roads. Table 1 shows the details of the nine typical road sites.

The rapid silt loading testing system was applied in the Tianjin urban area from January to October in 2015. Tianjin is a typical northern city with the monsoon climate found in the medium latitudes on the North China Plain, and thus January was a representative month in winter (December–February), and April, July, and October were representative months in spring (March–May), summer (June–August), and autumn (September–November), respectively. Therefore, sampling was conducted in January, April, July, and October.

RESULTS

Relationship between Vehicle Speed and Background-Corrected TRAKER Signals

Sixty data points were obtained in the speed response experiment described in Section 2.3. Fig. 2 shows the

Table 1. Details of roads sampled in this study.

Road name	Road type	Road direction
Weijin road	Major arterial	South-north direction
Fukang road	Major arterial	East-west direction
Huanghe road	Minor arterial	East-west direction
Anshan west road	Minor arterial	East-west direction
Erwei road	Branch road	East-west direction
Baidi road	Branch road	South-north direction
Yingshui road	Branch road	East-west direction
Hongqi road	Expressway	East-west direction
Waihuan west road	Outer ring	South-north direction

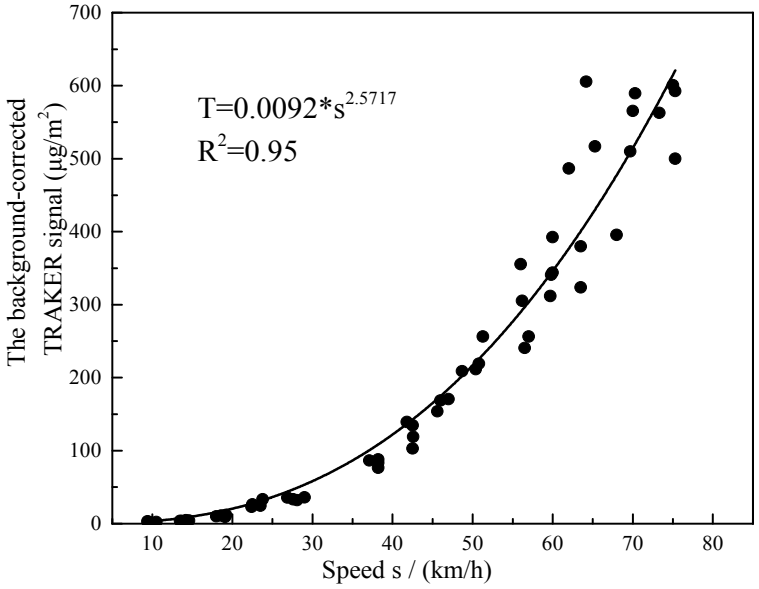

Fig. 2. Relationship between vehicle speed and background-corrected TRAKER signals.

relationship between the background-corrected TRAKER signals (T, mg m^{-3}) and vehicle speed (s, km h^{-1}), where each point represents the average value obtained by the TRAKER signal. T is the background-corrected TRAKER signal, which was obtained by subtracting the background-corrected values (mg m^{-3}) from the TRAKER signals measured behind the tire. The background-corrected values were obtained by subtracting the average TRAKER signals at a speed of 0 km h^{-1} from the background TRAKER signals. This accounted for particle losses within the TRAKER inlet lines, dust or exhaust emissions generated by other vehicles close to the TRAKER vehicle on the road, ambient wind, and inter-instrument bias. And the background-corrected values ranged from 0.000 to 0.012 mg m^{-3}.

Fig. 2 demonstrates that the background-corrected TRAKER signals increased with the vehicle speed over the same segment of road. The quantitative relationship between the background-corrected TRAKER signal and the vehicle speed was exponential, with a correlation coefficient (R^2) of 0.95 (about 95% of the variances in the signals were explained by the vehicle's speed). The correlations obtained by Etyemezian *et al.*(2003) between PM_{10} signals and vehicle speed in Treasure Valley and Ft Bliss speed tests were $T = 0.00017 \times s^{2.96}$ ($R^2 = 0.972$) and $T = 0.00012 \times s^{2.76}$ ($R^2 = 0.923$), respectively. There were some differences in these correlations, which may have been caused by the diverse silt and surface characteristics of the road sections sampled in the two studies. Therefore, when *sL* is measured in a specific area, the calibration procedure is essential in order to make the correlation equation applicable exclusively to local paved roads.

To remove the speed-dependent variable, the equation in Fig. 2 was transformed into another formula (formula (1)), where the average background-corrected TRAKER signals were adjusted to a speed of 40 km h^{-1}. We selected 40 km h^{-1} as the normalizing variable because this was the average speed during sampling.

$$T^* = \left(\frac{40}{S}\right)^{2.5717} \times T \quad (1)$$

where T is the background-corrected TRAKER signal in mg m^{-3}, s is the vehicle speed in the conventional units of km h^{-1}, and T^* is the speed-corrected TRAKER signal.

Relationship between the Speed-Corrected TRAKER Signals and sL Values

The regression equations obtained using the *sL* values (y) and speed-corrected TRAKER signals (x) in the four seasons are shown in Fig. 3, which indicates that the *sL* values increased exponentially with the speed-corrected TRAKER signals. The R^2 values for the four seasons were 0.901, 0.766, 0.584, and 0.768 respectively, which suggests that about 90%, 77%, 58%, and 77% of the variation in *sL* could be explained by the speed-corrected TRAKER signals in the four seasons, respectively. The equations presented in Fig. 3 were used to estimate the *sL* values based on the speed-corrected TRAKER signals on the scale of the whole study area. These results allowed us to establish the FRD *sL* reservoir in a more feasible manner on a higher geographic scale than that using *sL* measurements alone.

Spatial Distribution Characteristics of sL Values Obtained by TRAKER and its Impact Factors

Distribution Characteristics of the sL Values Obtained by TRAKER for Different Types of Roads and its Impact Factors

Fig. 4 shows the trends in the *sL* values obtained by TRAKER for various types of roads. As shown in Fig. 4, the average *sL* values obtained by TRAKER on different types of roads were 0.49 g m^{-2} for branch roads, 0.30 g m^{-2} for minor arterials, 0.29 g m^{-2} for major arterials, 0.26 g m^{-2} for the outer ring, and 0.09 g m^{-2} for the expressway. The maximum value (for branch roads) was five times the minimum (for the expressway) and there were obvious differences among the various types of roads. The average speeds on the different types of roads were as follows: expressway (53.72 km h^{-1}) > outer ring (48.69 km h^{-1}) > major arterials (36.42 km h^{-1}) > minor arterials (31.35 km h^{-1}) > branch roads (25.14 km h^{-1}). The trends in the traffic volumes were the same as the average speeds on the different types of roads, as shown in Table 2, so the traffic volume on the expressway was the maximum among all the types of roads in Tianjin. By contrast, the minimum traffic volume was found on the branch roads. Thus, the volume and speed were relatively lower on the branch roads than the others, so the FRD was more easily produced and its value was the maximum among all the types of roads. In addition, more crossings contributed to the maximum on branch roads because they led to more turning, braking, and starting, thereby increasing the maximum *sL* values determined by TRAKER. The main explanation for the minimum *sL* values on expressways was the higher traffic volume and average speed compared with the others, which led to a higher resuspension rate for the particles deposited on the road. There may also have been no major soil dust sources near the expressways, thereby leading to the minimum *sL* values determined by TRAKER. In addition, heavy trucks used for construction or transportation were found rarely on the expressway. In conclusion, the traffic volume and average speed were the major contributors to the *sL* values, but other factors could have influenced the *sL* values such as the road materials and road conditions (Zhu *et al.*, 2012). These results suggest that the *sL* values obtained by TRAKER were inversely proportional to both the average speed and traffic volume.

Based on those results, regulatory measures such as increasing the cleaning frequency should be taken to prevent the resuspension of FRD and maintain a clean and tidy road.

Distribution Characteristics of the sL Values Obtained by TRAKER in Different Vehicle Lanes

The *sL* values obtained by TRAKER in different vehicle lanes on various types of roads in Tianjin are shown in Fig. 6. A schematic diagram illustrating the different vehicle lanes on roads in Tianjin is shown in Fig. 5. Fig. 6 shows that the *sL* values obtained by TRAKER in slow lanes were

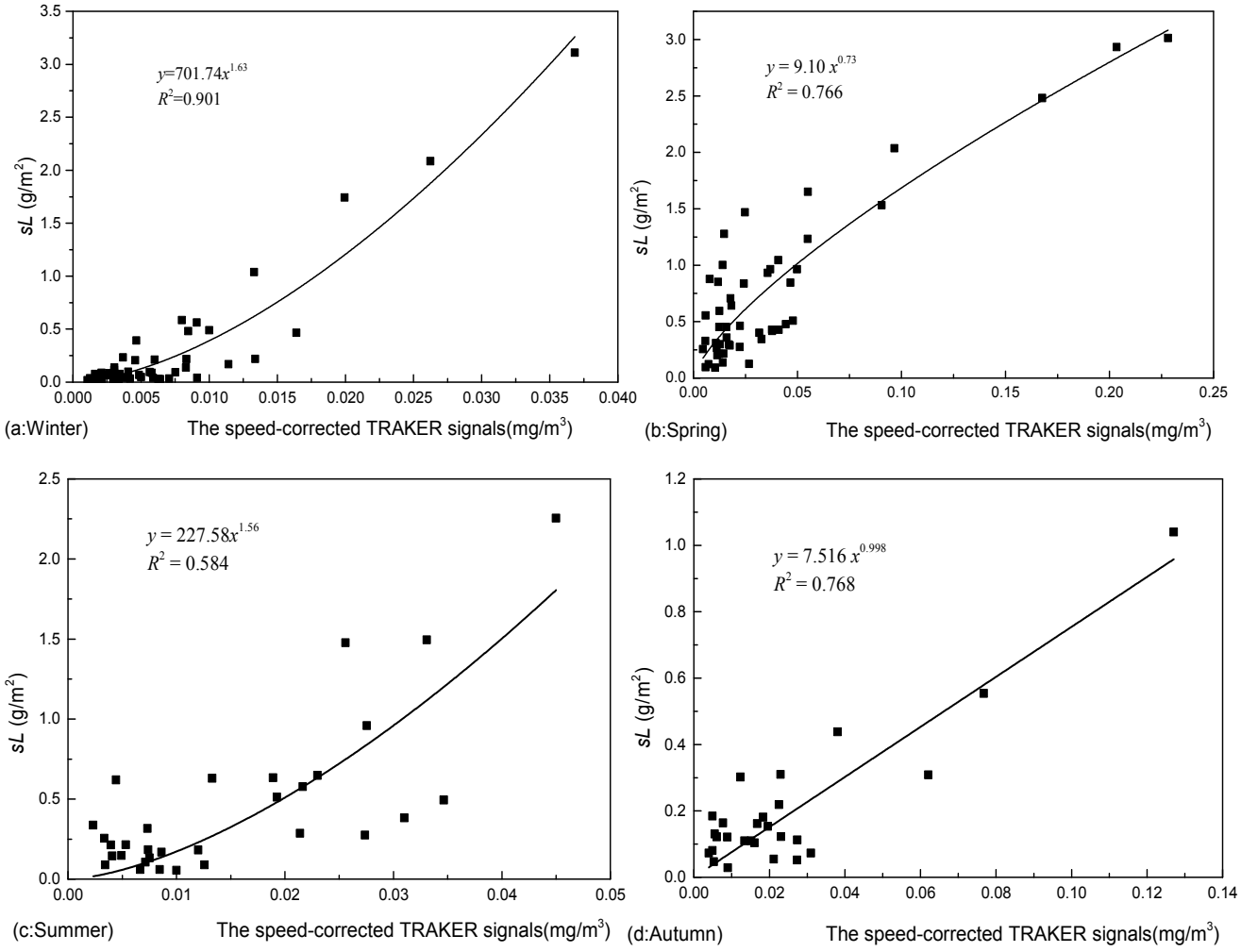

Fig. 3. Relationship between the speed-corrected TRAKER signals and *sL* values.

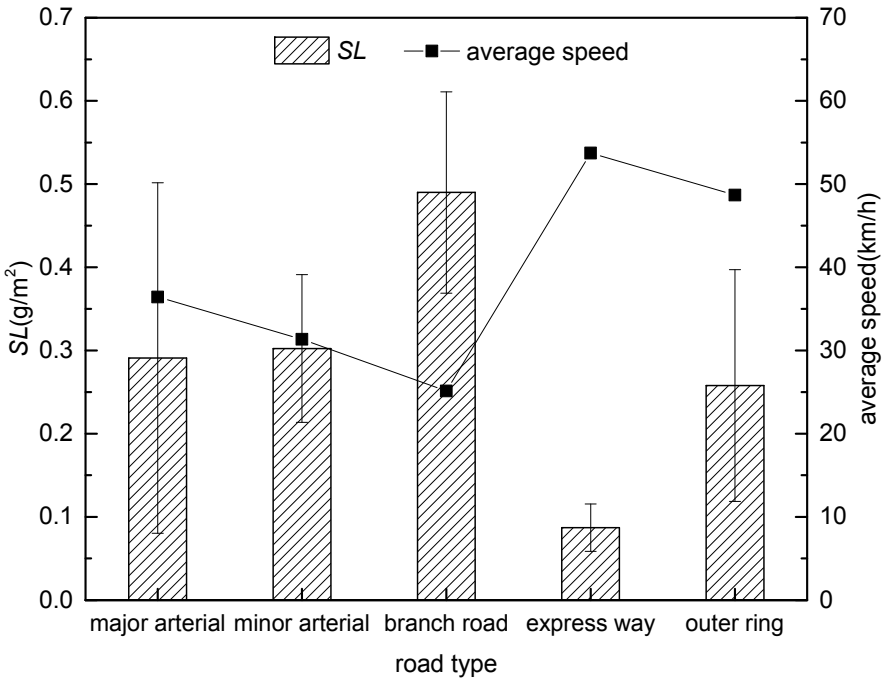

Fig. 4. *sL* values by TRAKER and the average speed on different types of roads.

Table 2. Traffic volume on various road types during sampling (unit: vehicles day^{-1}).

Road type	Major arterial	Minor arterial	Branch road	Expressway	Outer ring
Traffic volume	94,184	56,540	34,701	201,097	77,482

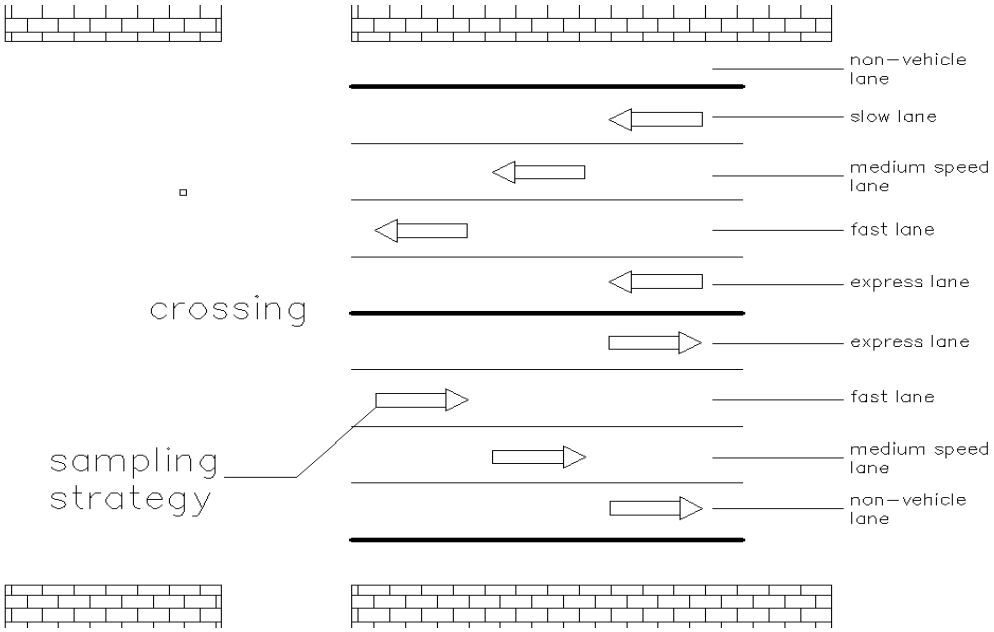

Fig. 5. Schematic diagram of different vehicle lanes on roads in Tianjin.

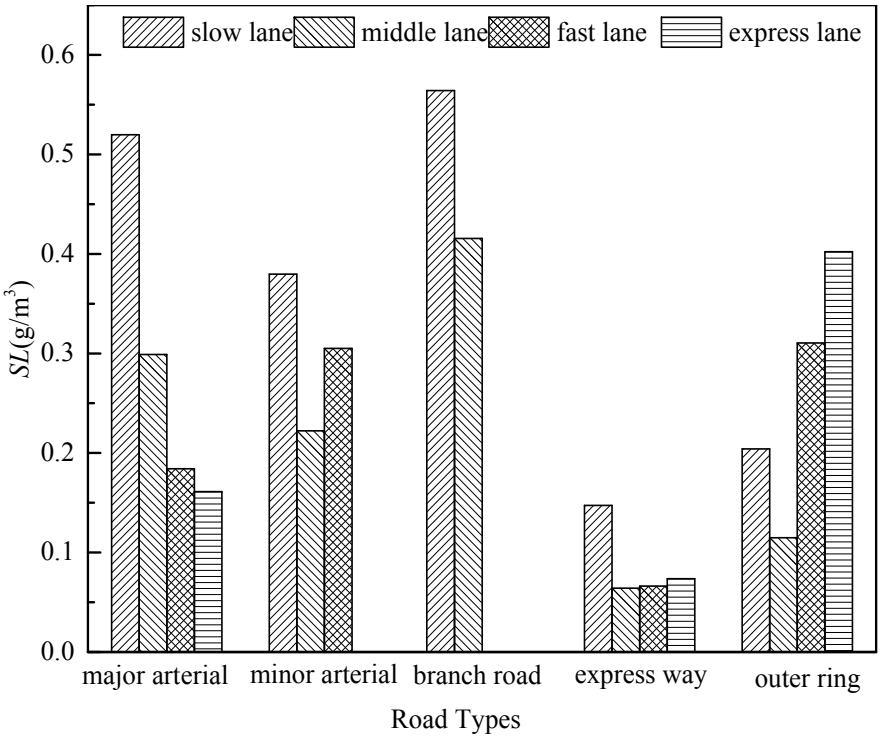

Fig. 6. *sL* values by TRAKER in different lanes on various types of roads in Tianjin.

higher than those in the other lanes (except for the outer ring), which may be associated with the minimum traffic volume and average speed in slow lanes. Fig. 6 shows clearly that there were no significant differences among lanes on the expressway (except for the slow lane), which might have been associated with their similar speed. However, the outer ring was a special type of road, where the traffic volume and speed did not differ significantly among lanes.

Furthermore, erosion due to rain and wind sent dust from the green belts into the nearby express lane, so the *sL* values obtained by TRAKER in this lane were higher than those in the others (Fig. 6). Thus the traffic volume and average speed were the main factors that affected the distribution of the *sL* values obtained by TRAKER in different lanes, as suggested previously (Han and Jung, 2012).

Frequency Distribution of sL Values Obtained by TRAKER on Different Types of Roads

Fig. 7 shows the frequency distribution of the *sL* values obtained by TRAKER on different types of roads. According to Fig. 7, the *sL* values determined by TRAKER on different types of roads were clearly quite different, especially on branch roads and minor arterials. For branch roads, about 34% of the *sL* values obtained by TRAKER were less than 0.2 g m^{-2} and about 5% were more than 1.0 g m^{-2}. For minor arterials, about 46% of the *sL* values obtained by TRAKER were less than 0.2 g m^{-2} and very few of the *sL* values were more than 1.0 g m^{-2}. For the five types of roads in Tianjin, the percentage of *sL* values obtained by TRAKER (< 0.2 g m^{-2}) on the expressway was relatively higher than that on any of the other types of roads (82%). Outer ring had the next highest percentage (60%), followed by major arterials (52%) and minor arterials (46%). The percentage of *sL* values obtained by TRAKER (< 0.2 g m^{-2}) was the lowest on branch roads (34%). Due to the high percentage range of *sL* values obtained by TRAKER (< 0.2 g m^{-2}) on different types of roads, many samples are required to ensure that accurate estimates are produced for *sL*. The results indicate that the frequency distribution of the *sL* values obtained by TRAKER was mainly related to the traffic volume and average speed.

The different frequency distributions indicated that there were significant differences among the types of roads and many measurements were needed to accurately estimate the *sL* values on an urban scale. The AP-42 method measures the *sL* based on a scale of only a small part of the road, thereby leading to greater uncertainty compared with the results obtained by TRAKER. Thus, the AP-42 method will lead to more uncertainty regarding the emission factors, and thus the emissions inventory.

Temporal Distribution of sL Values by TRAKER and its Impact Factors

The temporal distributions of the *sL* values obtained by TRAKER in different seasons are presented in Fig. 8, which suggests that there were seasonal differences among the *sL* values produced by TRAKER. The *sL* values obtained by TRAKER in summer were relatively higher than those in any of the other seasons (0.37 g m^{-2}). Spring was the next highest season (0.33 g m^{-2}), followed by autumn (0.26 g m^{-2}) and winter (0.24 g m^{-2}). As shown in Fig. 8, the days when the rainfall exceeded 0.254 mm in the four seasons followed the trend of: summer > autumn > spring > winter. The highest amount of rainfall in summer meant that the vehicle tires readily distributed mud on the road surfaces, thereby increasing the *sL* values for the road surface. Moreover, rainfall increased the accumulation of soil particles on the roads in rainwater from soil sources adjacent to the road

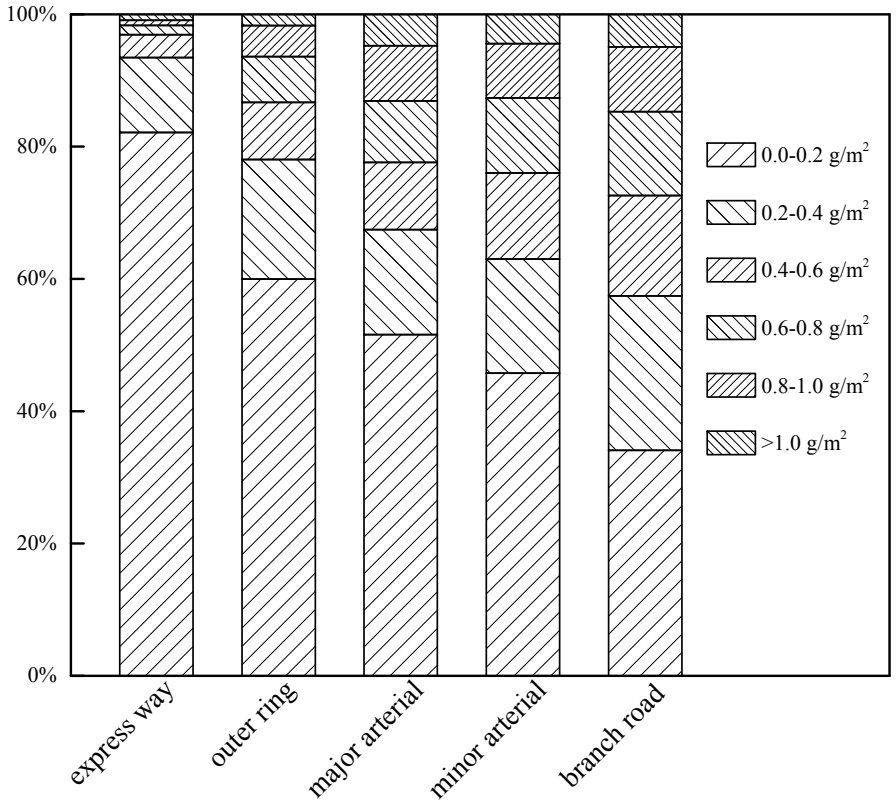

Fig. 7. Frequency distribution of the *sL* values by TRAKER on different types of roads.

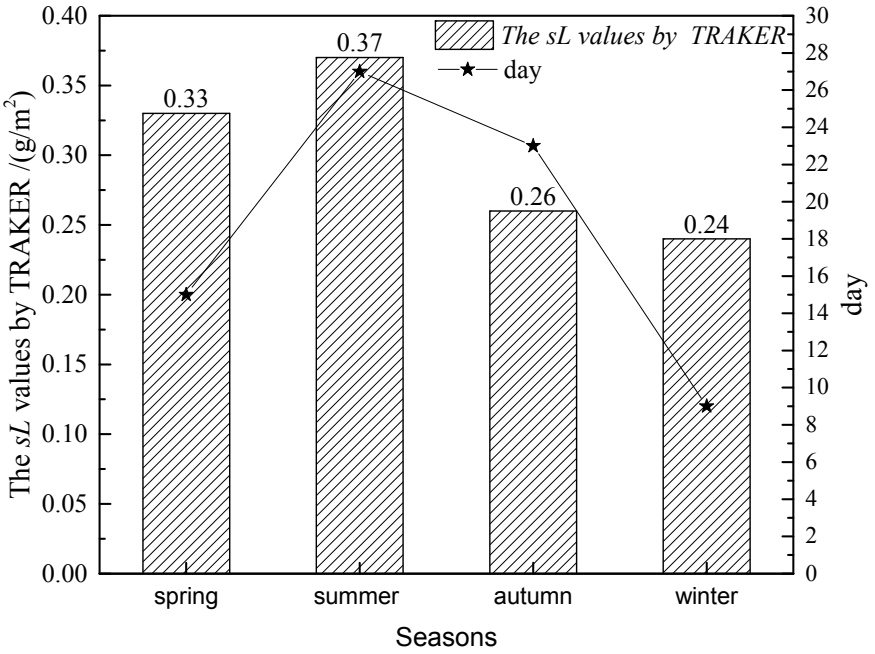

Fig. 8. Comparison of the *sL* values by TRAKER and the rainfall days in different.

during summer. The minimum *sL* values obtained by TRAKER in winter may be explained by the higher wind speed in winter among the four seasons, thereby increasing the FRD. Furthermore, the decreased fallout phenomenon during vehicle movements may be a factor that accounted for the minimum *sL* values obtained by TRAKER in winter. Therefore, the temporal distribution of the *sL* values obtained by TRAKER in different seasons may be related to many factors, such as temperature, humidity, rainfall, wind speed, and wind direction. Thus, more measures should be implemented, such as vacuum street sweeping and water spraying (Yuan *et al.*, 2003), to reduce the FRD levels during the summer and spring compared with the other two seasons.

CONCLUSIONS

This study obtained the first experimental estimations of road dust *sL* by using a rapid silt loading testing system in Tianjin. The rapid silt loading testing system combined TRAKER with AP-42, and it was implemented between January and October 2015 in Tianjin. The *sL* values were measured on typical roads during four seasons. After collecting sufficient data to determine the *sL* values using TRAKER, we determined the spatial and temporal distributions characteristics of the *sL* values, which allowed us to establish the FRD *sL* reservoir in a more feasible manner on an urban scale than that based on *sL* measurements obtained by AP-42 alone. This rapid silt loading testing system allows hot spots to be located easily and rapidly.

The background-corrected differential TRAKER signals increased slightly as the speed of the mobile monitoring system increased, and the *sL* values increased exponentially with the speed-corrected TRAKER signals. The *sL* values obtained by TRAKER were quite different among road types, i.e., branch roads > minor arterials > major arterials > outer ring > expressway, and they were inversely proportional to both the average speed and traffic volume. Furthermore, the *sL* values obtained by TRAKER in slow lanes were higher than those in the other lanes (except for the outer ring), and the *sL* values obtained by TRAKER in the express lanes of the outer ring were the highest among all the vehicle lanes. The frequency distributions of the *sL* values obtained by TRAKER were quite different among all types of roads in this study. Overall, our findings demonstrate that the traffic volume and average speed on roads were the main factors that determined the distribution characteristics of the *sL* values obtained by TRAKER.

The *sL* values obtained by TRAKER in summer were substantially higher than those in the other seasons. Spring was the next highest season, followed by autumn and winter. These differences may have been associated with the temperature, humidity, rainfall, wind speed, wind direction, and other meteorological factors.

ACKNOWLEDGMENTS

This study was funded by "Study on the measurement and emission detection of Road Dust in Beijing-Tianjin-Hebei Area" (2014-2016 Special Environmental Research Fund for Public Welfare, No. 201409004) from the Ministry of Environmental Protection of the People's Republic of China.

REFERENCES

Almeida, S.M., Pio, C.A., Freitas, M.C., Reis, M.A. and Trancoso, M.A. (2006). Source apportionment of atmospheric urban aerosol based on weekdays/weekend variability: Evaluation of road re-suspended dust contribution. *Atmos. Environ.* 40: 2058–2067.

Amato, F., Pandolfi, M., Escrig, A., Querol, X., Alastuey, A., Pey, J., Perez, N. and Hopke, P.K. (2009a). Quantifying road dust resuspension in urban environment by Multilinear Engine: A comparison with PMF2. *Atmos. Environ*. 43: 2770–2780.

Amato, F., Pandolfi, M., Viana, M., Querol, X., Alastuey, A. and Moreno, T. (2009b). Spatial and chemical patterns of PM_{10} in road dust deposited in urban environment. *Atmos. Environ.* 43: 1650–1659.

Amato, F., Nava, S., Lucarelli, F., Querol, X., Alastuey, A., Baldasano, J.M. and Pandolfi, M. (2010). A comprehensive assessment of PM emissions from paved roads: Real-world Emission Factors and intense street cleaning trials. *Sci. Total Environ.* 408: 4309–4318.

Amato, F., Karanasiou, A., Moreno, T., Alastuey, A., Orza, J.A.G., Lumbreras, J., Borge, R., Boldo, E., Linares, C. and Querol, X. (2012). Emission factors from road dust resuspension in a Mediterranean freeway. *Atmos. Environ*. 61: 580–587.

Amato, F., Favez, O., Pandolfi, M., Alastuey, A., Querol, X., Moukhtar, S., Bruge, B., Verlhac, S., Orza, J.A.G., Bonnaire, N., Le Priol, T., Petit, J.F. and Sciare, J. (2016). Traffic induced particle resuspension in Paris: Emission factors and source contributions. *Atmos. Environ.* 129: 114–124.

Athanasopoulou, E., Tombrou, M., Russell, A.G., Karanasiou, A., Eleftheriadis, K. and Dandou, A. (2010). Implementation of road and soil dust emission parameterizations in the aerosol model CAMx: Applications over the greater Athens urban area affected by natural sources. *J. Geophys. Res.* 115: D17301.

Borrego, C., Amorim, J.H., Tchepel, O., Dias, D., Rafael, S., Sá, E., Pimentel, C., Fontes, T., Fernandes, P., Pereira, S.R., Bandeira, J.M. and Coelho, M.C. (2016). Urban scale air quality modelling using detailed traffic emissions estimates. *Atmos. Environ*. 131: 341–351.

Cheng, S., Chen, D., Li, J., Wang, H. and Guo, X. (2007). The assessment of emission-source contributions to air quality by using a coupled MM5-ARPS-CMAQ modeling system: A case study in the Beijing metropolitan region, China. *Environ. Modell. Software* 22: 1601–1616.

Cyrys, J., Peters, A., Soentgen, J. and Wichmann, H.E. (2014). Low emission zones reduce PM_{10} mass concentrations and diesel soot in German cities. *J. Air Waste Manage. Assoc.* 64: 481–487.

Etyemezian, V. (2003). Vehicle-based road dust emission measurement (III): Effect of speed, traffic volume, location, and season on PM_{10} road dust emissions in the Treasure Valley, ID. *Atmos. Environ*. 37: 4583–4593.

Etyemezian, V., Kuhns, H., Gillies, J., Green, M., Pitchford, M. and Watson, J. (2003). Vehicle-based road dust emission measurement: I—methods and calibration. *Atmos. Environ*. 37: 4559–4571.

Fan, S., Tian, G., Li, G., Huang, Y., Qin, J. and Cheng, S. (2009). Road fugitive dust emission characteristics in Beijing during Olympics Game 2008 in Beijing, China. *Atmos. Environ.* 43: 6003–6010.

Gao, J., Peng, X., Chen, G., Xu, J., Shi, G.L., Zhang, Y.C. and Feng, Y.C. (2016). Insights into the chemical characterization and sources of $PM_{2.5}$ in Beijing at a 1-h time resolution. *Sci.Total Environ.* 542: 162–171.

Gopinath, K., Raj, M.B., Neethu, A.S. and Sivamoorthy, M. (2017). Source apportionment of $PM_{2.5}$ particles: Influence of outdoor particles on indoor environment of schools using Chemical Mass Balance. *Aerosol Air Qual. Res.* 17: 616–625.

Han, S., Youn, J.S. and Jung, Y.W. (2011). Characterization of PM_{10} and $PM_{2.5}$ source profiles for resuspended road dust collected using mobile sampling methodology. *Atmos. Environ*. 45: 3343–3351.

Han, S. and Jung, Y.W. (2012). A study on the characteristics of silt loading on paved roads in the Seoul metropolitan area using a mobile monitoring system. *J. Air Waste Manage. Assoc.* 62: 846–862.

Hsu, C.Y., Chiang, H.C., Lin, S.L., Chen, M.J., Lin, T.Y. and Chen, Y.C. (2016). Elemental characterization and source apportionment of PM_{10} and $PM_{2.5}$ in the western coastal area of central Taiwan. *Sci. Total Environ.* 541: 1139–1150.

Huang, R.J., Zhang, Y.L., Bozzetti, C., Ho, K.F., Cao, J.J., Han, Y.M., Daellenbach, K.R., Slowik, J.G., Platt, S.M., Canonaco, F., Zotter, P., Wolf, R., Pieber, S.M., Bruns, E.A., Crippa, M., Ciarelli, G., Piazzalunga, A., Schwikowski, M., Abbaszade, G., Schnelle-Kreis, J., Zimmermann, R., An, Z.S., Szidat, S., Baltensperger, U., El Haddad, I. and Prevot, A.S.H. (2014). High secondary aerosol contribution to particulate pollution during haze events in China. *Nature* 514: 218–222.

Hussein, T., Johansson, C., Karlsson, H. and Hansson, H.C. (2008). Factors affecting non-tailpipe aerosol particle emissions from paved roads: On-road measurements in Stockholm, Sweden. *Atmos. Environ*. 42: 688–702.

Karagulian, F., Belis, C.A., Dora, C.F.C., Prüss-Ustün, A.M., Bonjour, S., Adair-Rohani, H. and Amann, M. (2015). Contributions to cities' ambient particulate matter (PM): A systematic review of local source contributions at global level. *Atmos. Environ.* 120: 475–483.

Karanasiou, A., Moreno, T., Amato, F., Lumbreras, J., Narros, A., Borge, R., Tobías, A., Boldo, E., Linares, C., Pey, J., Reche, C., Alastuey, A. and Querol, X. (2011). Road dust contribution to PM levels – Evaluation of the effectiveness of street washing activities by means of Positive Matrix Factorization. *Atmos. Environ*. 45: 2193–2201.

Kauhaniemi, M., Stojiljkovic, A., Pirjola, L., Karppinen, A., Harkonen, J., Kupiainen, K., Kangas, L., Aarnio, M.A., Omstedt, G., Denby, B.R. and Kukkonen, J. (2014). Comparison of the predictions of two road dust emission models with the measurements of a mobile van. *Atmos. Chem. Phys.* 14: 9155–9169.

Kavouras, I.G., DuBois, D.W., Nikolich, G., Corral Avittia, A.Y. and Etyemezian, V. (2016). Particulate dust emission factors from unpaved roads in the U.S.–Mexico border semi-arid region. *J. Arid. Environ.* 124: 189–192.

Kuhns, H., Etyemezian, V., Landwehr, D., MacDougall, C., Pitchford, M. and Green, M. (2001). Testing Re-entrained Aerosol Kinetic Emissions from Roads: A new approach to infer silt loading on roadways. *Atmos.*

Environ. 35: 2815–2825.

Kwak, J., Lee, S. and Lee, S. (2014). On-road and laboratory investigations on non-exhaust ultrafine particles from the interaction between the tire and road pavement under braking conditions. *Atmos. Environ*. 97: 195–205.

Lai, S., Zhao, Y., Ding, A., Zhang, Y., Song, T., Zheng, J., Ho, K.F., Lee, S.C. and Zhong, L. (2016). Characterization of $PM_{2.5}$ and the major chemical components during a 1-year campaign in rural Guangzhou, Southern China. *Atmos. Res*. 167: 208–215.

Li, N., Long, X., Tie, X., Cao, J., Huang, R., Zhang, R., Feng, T., Liu, S. and Li, G. (2016). Urban dust in the Guanzhong basin of China, Part II: A case study of urban dust pollution using the WRF-Dust model. *Sci. Total Environ.* 541: 1614–1624.

Liu, E., Yan, T., Birch, G. and Zhu, Y. (2014). Pollution and health risk of potentially toxic metals in urban road dust in Nanjing, a mega-city of China. *Sci. Total Environ.* 476–477: 522–531.

Liu, G., Li, J., Wu, D. and Xu, H. (2015). Chemical composition and source apportionment of the ambient $PM_{2.5}$ in Hangzhou, China. *Particuology* 18: 135–143.

Long, X., Li, N., Tie, X., Cao, J., Zhao, S., Huang, R., Zhao, M., Li, G. and Feng, T. (2016). Urban dust in the Guanzhong Basin of China, Part I: A regional distribution of dust sources retrieved using satellite data. *Sci. Total Environ.* 541: 1603–1613.

Lu, H.Y., Mwangi, J.K., Wang, L.C., Wu, Y.L., Tseng, C.Y. and Chang, K.H. (2016). Atmospheric $PM_{2.5}$ characteristics and long-term trends in Tainan city, southern Taiwan. *Aerosol Air Qual. Res*. 16: 2488–2511.

Lu, X., Li, L.Y., Wang, L., Lei, K., Huang, J. and Zhai, Y. (2009). Contamination assessment of mercury and arsenic in roadway dust from Baoji, China. *Atmos. Environ.* 43: 2489–2496.

Martuzevicius, D., Kliucininkas, L., Prasauskas, T., Krugly, E., Kauneliene, V. and Strandberg, B. (2011). Resuspension of particulate matter and PAHs from street dust. *Atmos. Environ.* 45: 310–317.

Moreno, T., Karanasiou, A., Amato, F., Lucarelli, F., Nava, S., Calzolai, G., Chiari, M., Coz, E., Artíñano, B., Lumbreras, J., Borge, R., Boldo, E., Linares, C., Alastuey, A., Querol, X. and Gibbons, W. (2013). Daily and hourly sourcing of metallic and mineral dust in urban air contaminated by traffic and coal-burning emissions. *Atmos. Environ.* 68: 33–44.

Sindhwani, R., Goyal, P., Kumar, S. and Kumar, A. (2015). Anthropogenic emission inventory of criteria air pollutants of an urban agglomeration - National Capital Region (NCR), Delhi. *Aerosol Air Qual. Res*. 15: 1681–1697.

Sumit, S. and Kavita, V.P. (2016). Emission scenarios and health impacts of air pollutants in Goa. *Aerosol Air Qual. Res*. 16: 2474–2487.

Sun, Y., Zhuang, G., Wang, Y., Han, L., Guo, J., Dan, M., Zhang, W., Wang, Z. and Hao, Z. (2004). The air-borne particulate pollution in Beijing—concentration, composition, distribution and sources. *Atmos. Environ.* 38: 5991–6004.

Tente, H., Gomes, P., Ferreira, F., Amorim, J.H., Cascão, P., Miranda, A.I., Nogueira, L. and Sousa, S. (2011). Evaluating the efficiency of Diesel Particulate Filters in high-duty vehicles: Field operational testing in Portugal. *Atmos. Environ.* 45: 2623–2629.

Thorpe, A. and Harrison, R.M. (2008). Sources and properties of non-exhaust particulate matter from road traffic: A review. *Sci. Total Environ.* 400: 270–282.

Tian, Y.Z., Chen, G., Wang, H.T., Huang-Fu, Y.Q., Shi, G.L., Han, B. and Feng, Y.C. (2016). Source regional contributions to $PM_{2.5}$ in a megacity in China using an advanced source regional apportionment method. *Chemosphere* 147: 256–263.

Yuan, C.S., Cheng, S.W., Hung, C.H. and Yu, T.Y. (2003). Influence of operating parameters on the collection efficiency and size distribution of street dust during street scrubbing. *Aerosol Air Qual. Res.* 3: 75–81.

Zhao, H., Shao, Y., Yin, C., Jiang, Y. and Li, X. (2016). An index for estimating the potential metal pollution contribution to atmospheric particulate matter from road dust in Beijing. *Sci. Total Environ.* 550: 167–175.

Zhao, P., Feng, Y., Zhu, T. and Wu, J. (2006). Characterizations of resuspended dust in six cities of North China. *Atmos. Environ.* 40: 5807–5814.

Zhu, D., Kuhns, H.D., Brown, S., Gillies, J.A., Etyemezian, V. and Gertler, A.W. (2009). Fugitive dust emissions from paved road travel in the Lake Tahoe basin. *J. Air Waste Manage. Assoc.* 59: 1219–1229.

Zhu, D., Kuhns, H.D., Gillies, J.A., Etyemezian, V., Brown, S. and Gertler, A.W. (2012). Analysis of the effectiveness of control measures to mitigate road dust emissions in a regional network. *Transp. Res. Part D* 17: 332–340.

Received for review, December 30, 2016
Revised, April 11, 2017
Accepted, May 12, 2017